# Dielectric and impedance spectroscopic studies of multiferroic BiFe$_{1-x}$Ni$_x$O$_3$

## M. R. Biswal[1], J. Nanda[2*], N. C. Mishra[3], S. Anwar[4], A. Mishra[4]

[1]*Department of Physics, Jupiter +2 Science College, Bhubaneswar, Odisha, India*
[2]*Department of Physics, I.T.E.R., Siksha 'O' Anusandhan University, Bhubaneswar, Odisha, India*
[3]*Department of Physics, Utkal University, Bhubaneswar, Odisha, India*
[4]*Institute of Materials and Minerals Technology, Bhubaneswar, Odisha, India*

[*]Corresponding author. Tel: (+91) 9437951178; E-mail: jnanda_b9@rediffmail.com

## ABSTRACT

Multiferroic bismuth ferrites (BFO) and Ni substituted bismuth ferrites (BFNO) were synthesized by standard solid state reaction route. The structural and microstructural studies were carried out. The effect of Ni substitution on dielectric constant and dielectric loss of the samples was studied in a wide range of frequency (100 Hz- 1 MHz) and temperature (27 $^o$C – 420 $^o$C). It has been observed that the dielectric constant increases with increase in Ni doping concentration and attained a maximum value for BFNO(x = 0.075) sample while the dielectric loss has been found to decrease with the doping concentration. This implies a reduction in the conductivity and hence improved the dielectric properties of Ni doped BFO. The anomalous peaks in temperature dependent dielectric studies indicate the increase in antiferromagnetic ordering temperature and possible existence of spin glass states upon Ni substitution in place of Fe. The complex impedance spectroscopic analysis suggests purely the intrinsic nature of the dielectric anomalies. Temperature dependent non-Debye type of dielectric relaxation has also been observed. The Nyquist plots show the negative temperature coefficient of resistance behavior of these compounds. Further it would be interesting to study their magnetic and magnetoelectric properties with the aim of identifying new multifunctional device applications. Copyright © 2014 VBRI press.

**Keywords:** Ceramics; microstructure; dielectric response; complex impedance spectroscopy.

**Manas Ranjan Biswal** is a research scholar in the Department of Physics in the Siksha 'O' Anusandhan University, Bhubaneswar, Odisha, India. He is presently working as senior lecturer in physics at Jupiter Science College Bhubaneswar, Odisha, India. His active area of research interest is the synthesis and characterization of multiferroic ceramics.



**Jyotirmayee Nanda** is presently working as associate professor in the department of physics, institute of technical education and research, Siksha 'O' Anusandhan University, Odisha, India. She did her MSc, MPhil in Physics from Utkal University and Ph.D. (1998) in the area of magnetic thin films from IIT Mumbai, India. Her present research interest includes synthesis and study on multiferroic materials, ferrite thin films and nanocomposites for device applications.



**N. C. Mishra** is a Professor and Head of the PG Department of Physics, Utkal University, Bhubaneswar, India. His research interests include synthesis and study of nanoparticle thin films and bulk materials and evolution of materials under irradiation by high energy heavy ions. He is the Chairman of the Accelerator Users Committee of the Inter-University Accelerator Centre, New Delhi and member of many National Research Committees. He has published more than 100 research articles in journals of International/ National repute and has completed many research projects funded by DST, UGC, IUAC and UGC-DAE CSR.

## Introduction

Multiferroic materials display simultaneous presence of two or all three primary ferrioc properties like ferromagnetism/ antiferromagnetism, ferroelectricity/ antiferroelectricity and ferroelasticity **[1]**. Additionally, they exhibit the phenomenon called magnetoelectric coupling, i.e. magnetization induced by an electric field and electric polarization induced by a magnetic field. These materials have attracted a lot of attention in recent years due to their

potential applications in multiple state memory elements, spintronics, electric field controlled ferromagnetic resonance devices, microelectronic devices, transducers etc [2-4]. Amongst the multiferroic materials, there have been intensive studies on $BiFeO_3$ (BFO) due to its multiferroic properties at room temperature (RT) [5]. BFO is a rhombohedrally distorted perovskite material with space group R3c at RT with a high ferroelectric Curie temperature ($T_C \sim 830°C$) and G-type antiferromagnetic Neel temperature ($T_N \sim 370°C$). [2, 6]. The BFO samples usually show high leakage current which prohibits getting a well saturated P-E hysteresis loop. Therefore, there have been constant efforts to reduce the leakage current, improvements in the dielectric and magnetic properties by substitutions on Bi-site and/or Fe-site [7-10]. The enhancements in both dielectric constant and dielectric loss have been reported [11] in Nd and La doping BFO ceramics. Research is still being carried out in the substituted BFO ceramics to fabricate a high dielectric constant material with temperature and frequency independence characteristics for miniaturization in electronic devices.

In this regard, attempts have been made to substitute the transition metal ion, $Ni^{2+}$ (similar ion size as $Fe^{3+}$) on Fe-site to improve upon the magnetic, dielectric and magnetoelectric properties of BFO ceramics [12-18] and BFO thin films [19]. The resistivity of Ni doped BFO was reduced by more than three orders of magnitude than the un-doped BFO [15]. The doping of $Ni^{2+}$ is expected to prevent the formation of $Fe^{2+}$. It may introduce more oxygen vacancies that leads to a higher density of free carriers and hence higher conductivity [20]. Singh et al. have reported a structural change in their Ni doped BFO films grown by chemical-solution deposition on $Pt/Ti/SiO_2/Si(100)$ substrate [14]. Films with 2.5 atom % Ni substitution showed low leakage current with high polarization and coercive field in the PE hysteresis loops. It has also been reported that the presence of microstructural defects or grain boundaries may be primarily responsible for determining the magnetic and electrical properties of transition metal doped BFO thin films [19].

In this paper, synthesis of BFO and Ni substituted BFO (BFNO) ceramics by solid state reaction route is reported. A thorough study on the effect of $Ni^{2+}$ substitution on structural, micro structural and dielectric properties has been carried out. The complex impedance spectroscopic data has been analyzed to understand the electrical properties of these materials. So far as author's knowledge is concerned, this article may be the first report on a thorough study on the dielectric properties and complex impedance analysis of the Ni doped bismuth ferrites.

## Experimental

### Materials

High purity powders of $Bi_2O_3$ (3 mol% $Bi_2O_3$ excess), $Fe_2O_3$, and NiO (all are of purity $\geqq 99\%$, Merck) were used as starting materials. The chemicals were of analytical grades.

### Synthesis

Polycrystalline $BiFe_{1-x}Ni_xO_3$(x = 0, 0.025, 0.05, 0.075, 0.10, 0.15, 0.20) ceramics were synthesized by the standard solid state reaction technique. The above materials were carefully weighed in stoichiometric proportion and thoroughly mixed by grinding in ethanol medium for 2 hours using agate mortar and pestle. This homogeneous mixture was rapidly heated to 800 °C and calcinated there for two hours. Calcined powder was again ground thoroughly for 30 minutes. The powder was then pressed into pellets of 10 mm diameter and 1-1.5 mm thickness by applying a pressure of 1 MPa (with PVA as a binder). The pellets were rapidly heated to 800 °C and sintered for 2 hours. The sintered BFO pellets were found to be grey in colour but the colour changed to dark grey upon Ni substitution.

### Characterizations

The crystallinity and phase of the samples were examined by X-ray diffraction (XRD, Bruker D8 Advance, Germany), using Cu Kα radiations (λ = 1.5406 Å) in 2θ ranging from 20 ° to 60°. The dielectric measurements and complex impedance spectroscopic analysis were carried out as a function of frequency (100 Hz – 1 MHz) and temperature (300 K – 723 K) using a LCR meter (model-PSM1735 HIOKI ). Prior to this measurement, silver paste was applied on the opposite faces of the sintered pellets for good electrical contacts. Scanning electron microscopy (SEM, Model: JEOL-JEM 2100 UHR) was used to study the surface morphology of the samples.

## Results and discussion

### Structural analysis

The X-ray diffraction patterns of BFO and BFNO ceramics are illustrated in **Fig. 1**. The XRD peaks were indexed with a rhombohedrally distorted perovskite structure with space group *R*3c. Nickel doping up to 15 % did not cause a change in structure. No new peaks were observed corresponding to any phase associated with Ni. These observations indicate that Ni ions are incorporated into the BFO structure. Weak secondary phase peaks like $Bi_2Fe_4O_9$ and $Bi_{25}FeO_{40}$ were observed along with main peaks. These phases are usually observed in BFO and substituted BFO samples because of the kinetics of formation [8, 21, 22]. Intensity of some of the diffraction peaks corresponding to secondary phases decreased with increasing Ni concentration (up to 0.075) and increased thereafter (up to 0.20). The effect of Ni doping at low concentrations in suppressing impurity phases has also been reflected in the dielectrics data as discussed later.

The effect by Ni substitution on the morphology and shape of the grains was studied by SEM analysis. SEM images of samples with $Ni_x$ (x= 0, 0.075, 0.10, 0.15) are shown in **Fig. 2**. Most of the grains are homogeneous with an individual grain size of approximately 0.5 μm. However a few large grains of irregular shapes were also observed. The variation of grain morphologies may be an evidence of the formation of secondary phases.
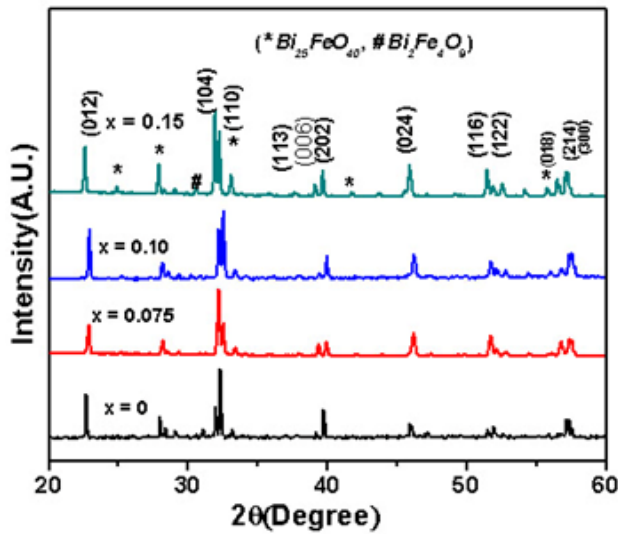
**Fig.1.** X-ray diffraction (XRD) patterns of $BiFe_{1-x}Ni_xO_3$ ceramics; '*' and '#' correspond to the impurity peaks.
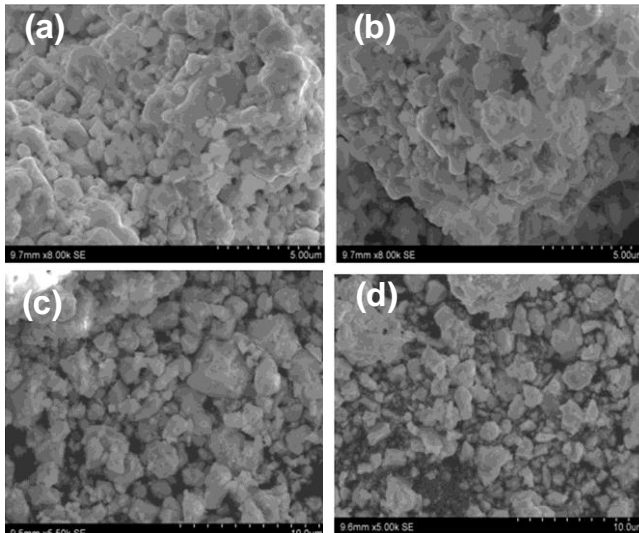


**Fig. 2.** Scanning electron microscope (SEM) images of $BiFe_{1-x}Ni_xO_3$ samples where **(a)** $x = 0$, **(b)** x= 0.075, **(c)** x= 0.10 and **(d)** x= 0.15.

*Dielectric study*

The dielectric constant ($\varepsilon_r$) and dielectric loss ($tan\delta$) of BFO and BFNO ceramics exhibited strong dependence on frequency (**Fig. 3**). The occurrence of dispersion in the low frequency regime may be attributed to interfacial polarization [23]. This also indicates the presence of dc conductivity in BFO and doped BFO [24, 25].

As shown in **Fig. 3**(**a**), the values of dielectric constant are very high at low frequencies. This phenomenon has been understood on the basis of space charge polarization due to the presence of porosity. Initially, the $\varepsilon_r$ values for all the samples initially showed a sharp decrease up to 10 kHz and thereafter the decrease was found to be slow and became almost constant up to a frequency of 1 MHz. This observed trend of decrease in dielectric constant with increased frequency may be attributed to the inability of the electric dipoles to be influenced by the applied field. This type of behavior has been reported for Co doped [26], Cr doped [27] and Ni doped [28] BFO samples. It was also

observed that the dispersion in $\varepsilon_r$ values with Ni doping concentration was more at low frequency region than that at the high frequency region.
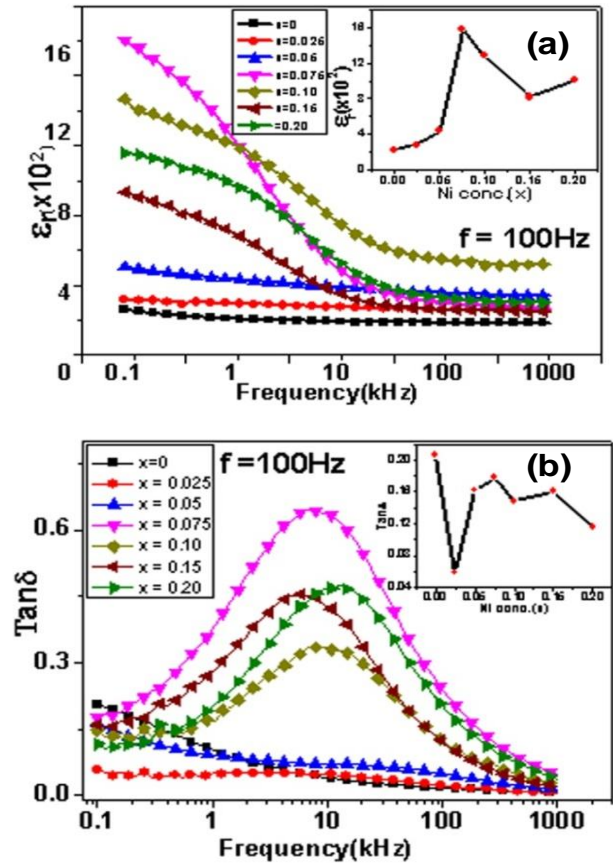


**Fig. 3.** Frequency dependence of the dielectric constant ($\varepsilon_r$) **(a)** and dielectric loss ( $tan\delta$ ) **(b)** of $BiFe_{1-x}Ni_xO_3$ ceramics at room temperature. The insets show the variation of $\varepsilon_r$ and $tan\delta$ with Ni concentration at 0.1 kHz.

This weak dependence of $\varepsilon_r$ on frequency at high frequency region could be due to the contributions from ferroelectric domains rather than the dipoles.

The inset of **Fig 3(a)** shows the variation of dielectric constant with Ni concentration at a frequency of 100 Hz. The dielectric constant for BFO sample was found to be low but increased with increasing in Ni doping concentration. It became maximum for BFNO(x = 0.075), almost eight times as compared to BFO. This significant increase in the dielectric values may be attributed to the reduction in the impurity phases. XRD spectra (**Fig. 1**) also showed the reduced intensity of the impurity peaks at this Ni substitution. This behavior might also be understood in terms of oxygen vacancies and displacement of $Fe^{3+}$ ions.

**Fig. 3(b)** shows the dielectric loss as a function of frequency. The dielectric loss of BFO sample decreased with increasing frequency and was owing to the suppressed dipolar contribution towards the polarization at high frequencies [7]. For the BFNO samples with x= 0, 0.025 and 0.05, a broad peak appeared at around 10 kHz. The peak was prominent in loss tangent curves of BFNO (x= 0.075-0.2) almost at the same frequency. The occurrence of broad relaxation peak was also reported for La doped BFO samples [29]. This could be attributed to non-Debye type

relaxations, which might arise due to space charge conduction. The hopping motion of the double ionized oxygen ion vacancies [30] (among the potential barriers) could also play a role in causing such type of relaxation. The variation of dielectric loss with Ni concentration at 100 Hz is shown in inset of **Fig. 3(b)**. The dielectric loss was observed to decrease with the doping concentration. This implies a reduction in the conductivity, thus improving dielectric properties of Ni doped BFO.

**Fig. 4(a)** shows the variation of dielectric constant with temperature of BFO and BFNO ceramics measured at 10 kHz frequency. The dielectric values of the BFO sample were found to be small in the entire temperature range, except a high dielectric constant peak at a temperature of 350 $^{\circ}$C. Such dielectric anomaly has already been reported for phase pure BFO samples [31, 32]. Usually this anomaly is observed at around the antiferromagnetic Neel temperature (i.e. 370 $^{\circ}$C for BFO), which is much lower than the ferroelectric transition temperature (870 $^{\circ}$C). Hence, the observed anomaly could be attributed to the magnetoelectric coupling, which caused a change in the electric polarization. The Landau-Devenshire theory of phase transitions has predicted such type of dielectric anomaly in magnetoelectrically ordered system [33]. The position of this anomaly peak shifted towards a higher temperature i.e. 400 $^{\circ}$C with the substitution of Ni into the BFO lattices. This indicated about the increase in antiferromagnetic ordering temperature upon Ni substitution.
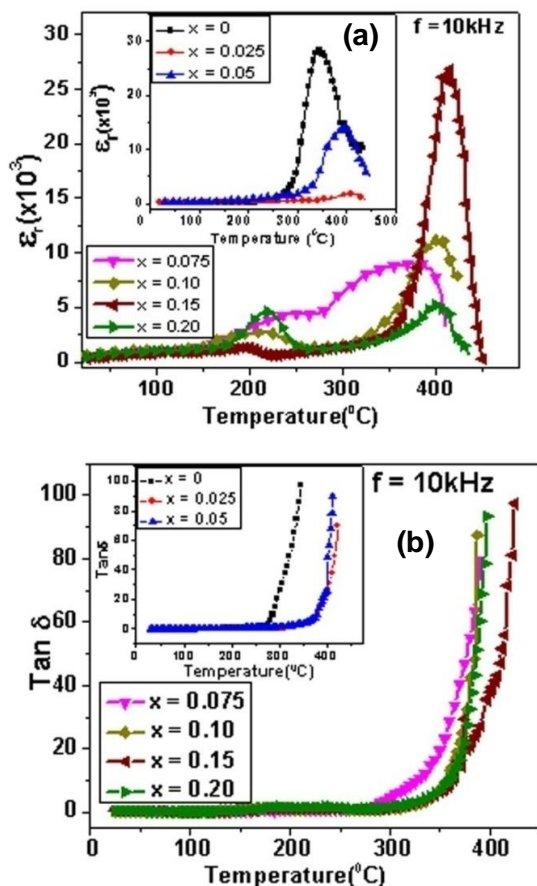
Dielectric constant versus temperature plot of BFNO(x = 0.075 to x=0.20) exhibited one additional anomaly peak at around 220$^{\circ}$C. Such type of behavior has also been reported previously by several authors [16, 34-38]. The existence of anomaly in the temperature range 200 $^{\circ}$C to 220 $^{\circ}$C might be attributed to the development of another magnetic transition (spin-glass like behavior) [39], which needs a thorough investigation on the magnetic properties of these samples.

**Fig. 4(b)** shows the effect of temperature on dielectric loss of BFO and BFNO samples. It was observed that the value increased steeply after 300 $^{0}$C. This may be understood as follows. There is always some contribution of space charge polarization due to oxygen ion vacancies in the BFO and doped BFO samples in the entire temperature range. But at higher temperature this effect becomes more prominent due to thermally activated process, which enhances the loss tangent to very high value. This type of behavior has been reported for La and Nb co-doped BFO [40], La and Ho co-doped BFO[41] and Ti doped BFO [8].

*Complex impedance spectroscopy*

**Fig. 5** shows the variation of real part ($Z^{'}$) and imaginary part ($Z^{''}$) of impedance of BFO and BFNO with frequency at room temperature. The magnitude of $Z^{'}$ was found to be high at low frequency region. With increase in frequency, $Z^{'}$ decreased monotonically and attained a constant value in the high frequency region. This type of trend was exhibited by BFO and all BFNO samples without any signature of anomalous behaviour. The values of $Z^{'}$ and $Z^{''}$ were observed to merge above 10 kHz. This trend could be understood by the increased hopping of charge carriers between the localized ions and conductivity across grain boundaries at high frequencies. Moreover, the magnitude of $Z^{'}$ gradually decreased with the Ni concentration. This indicated the decrease in conduction path due to lattice distortion
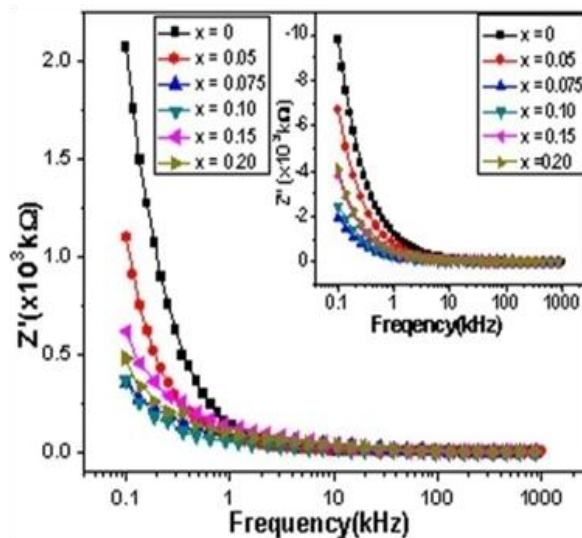


**Fig.4.** (a)Temperature dependence of the dielectric constant($\varepsilon_r$) and (b) dielectric loss ( $tan\delta$) of $BiFe_{1-x}Ni_xO_3$ at 10 kHz.



**Fig. 5.** The real ($Z^{'}$) and imaginary components ($Z^{''}$) of impedance of $BiFe_{1-x}Ni_xO_3$ at room temperature.

**Fig. 6** shows the frequency dependence of $Z'$ and $Z''$ at different temperatures. As shown in the figure, $Z'$ decreased with a rise in temperature and merged at high frequency region due to the increase of ac conductivity. This indicates the existence of negative temperature coefficient of resistance (NTCR) in the compounds, usually observed in semiconductors. Decrease of $Z'$ with increase of temperature and frequency has been reported by several authors, where they have suggested a possible release of space charge and consequently lowering of barrier properties in these materials [42, 43].
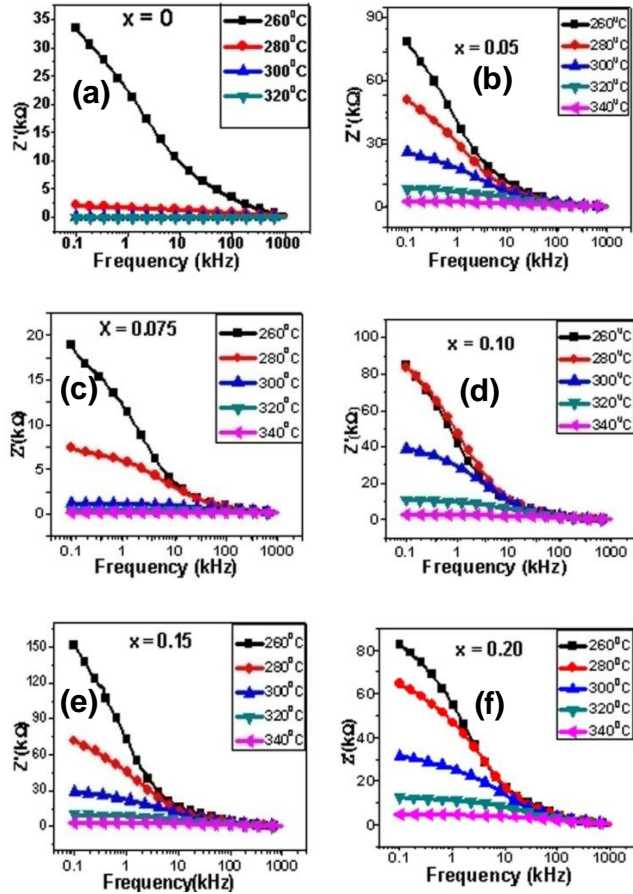
**Fig. 6.** Variation of $Z'$ with frequency of $BiFe_{1-x}Ni_xO_3$ samples at selected temperatures.

**Fig. 7** shows the variation of imaginary part of impedance ($Z''$) with frequency (known as loss spectrum) at various temperatures. The appearance of peaks suggested the existence of relaxation properties of these materials. It is known that these peaks appear when the hopping frequency of localized electrons becomes approximately equal to the frequency of applied field. The occurrence of relaxation peaks could be understood by the presence of immobile species/electrons at low temperatures and defect/vacancies at high temperature [44]. The broadening of peaks at higher temperatures confirmed the existence of temperature dependent electrical relaxation phenomena in these materials. Moreover, the peak was found to be shifted towards higher frequency side by the rise in temperature. The magnitude of $Z''$ was found to be almost independent of temperature at a frequency of 1 MHz. This may be

understood by the disappearance of space charge polarization at high frequency [42, 44].
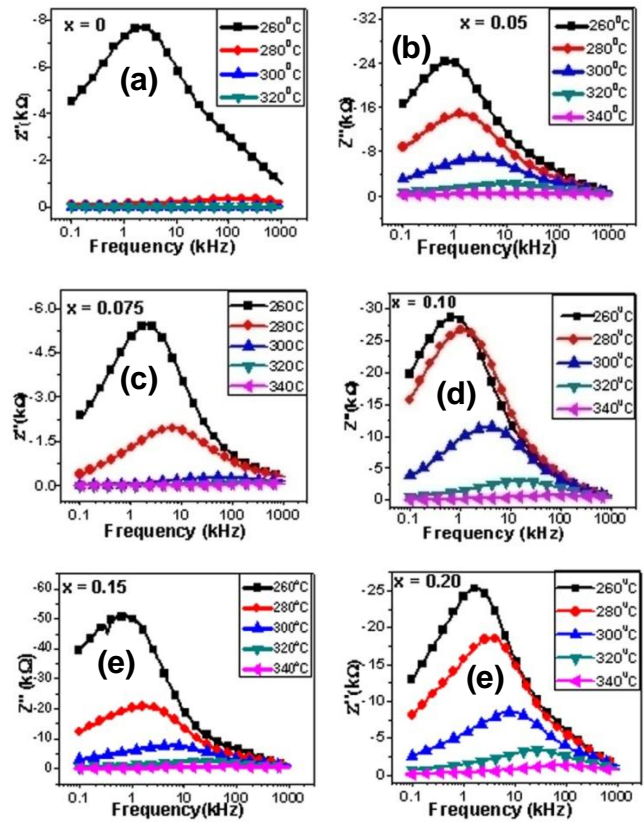
**Fig. 7.** Variation of $Z''$ with frequency of $BiFe_{1-x}Ni_xO_3$ samples at selected temperatures.

The temperature dependence of complex impedance spectrum $Z'$ vs $Z''$ (called as Nyquist Plot) of BFNO is displayed in **Fig. 8**. At low temperature (below $300^0C$ approx.), the complex impedance plots of all samples consist of two overlapping semicircular arcs with centre below the real axis. This showed the presence of non-Debye type of relaxation phenomenon in the samples. At above $300^0C$, a semicircular arc with some missing portion was observed at low frequency region due to limitation of our experimental facilities (inset in **Fig. 8**).

The small semicircular arc (low frequency) is attributed to grain boundary effects and the large semicircular arcs (high frequency) are attributed to the bulk (grain) effect. The values of bulk resistance ($R_b$) were calculated from the intercept of the impedance curve to the $Z''$-axis. The values of $R_b$ showed a decreasing trend with increase of temperature. This also indicates a typical NTCR behaviour of the BFNO compounds.

Moreover, the intrinsic capacitance of the compounds in the high frequency range $10^4$ to $10^6$ Hz was extracted from the equivalent circuit of the impedance spectrum, using $-Z'' = \frac{1}{jC_b \times \omega}$. Where $j = \sqrt{-1}$, $\omega$ is the angular frequency ($\omega = 2\pi f$) and $C_b$ is the bulk capacitance. The magnitude of $C_b$ could be calculated from the slope of the plot between $-Z''$ vs. $1/2\pi f$ as shown in the **Fig. 9** (inset). The variation of intrinsic capacitance with temperature of BFNO (x=0.15) sample is displayed in **Fig. 9**. This Figure clearly indicates the presence of the anomalies at 200 °C

and 400 $^o$C, which is similar to that observed in **Fig. 4(a)**). Therefore, it may be concluded that the observed dielectric anomalies are purely intrinsic in nature.
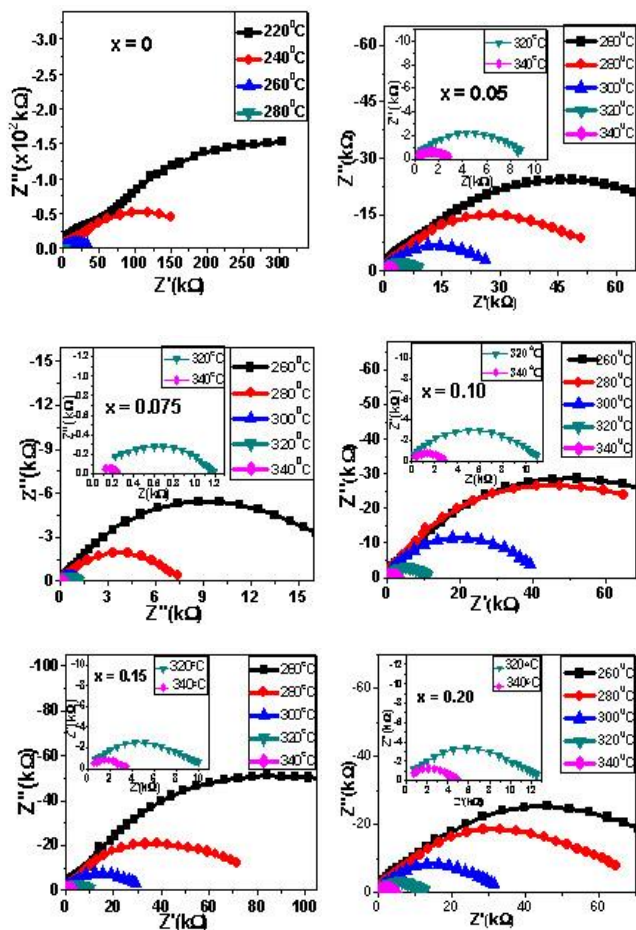


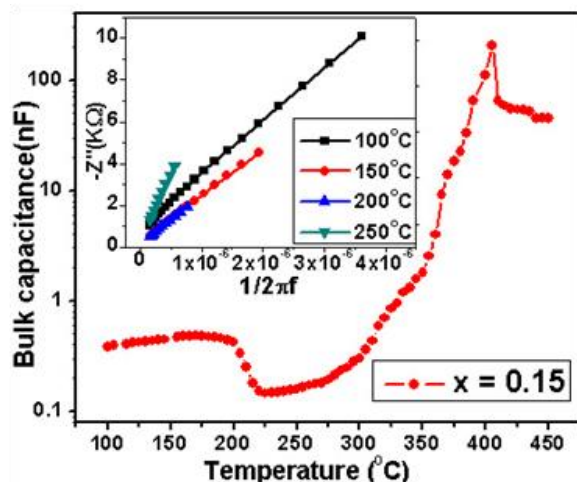**Fig. 8.** Complex impedance spectra ($Z''$ vs $Z'$) of $BiFe_{1-x}Ni_xO_3$ samples at selected temperatures.



**Fig. 9.** Temperature vs bulk capacitance of $BiFe_{0.85}Ni_{0.15}O_3$ and inset showing frequency vs $Z''$.

Majumdar et al., **[38]** have also reported the intrinsic nature of the dielectric anomalies in their study on BFO samples. They have ruled out the possible existence of the extrinsic factors such as electrode-sample interface or the grain boundaries.

## Conclusion

Nickel substituted BFO ceramics were prepared by solid state reaction technique. The influences of the Ni doping content on the crystallization and dielectric properties of the samples were investigated. XRD studies showed that the rhombohederal distorted perovskite structure of the parent compound was retained even with Ni concentration 15%. The surface morphology of the compound was studied through SEM, which revealed the average grain size of the order of 0.5 μm. The dielectric measurements showed that the values of dielectric constants were very high at low frequency region. The dielectric constant was found to decrease with increase in frequency, whereas peaks (non-Debye type of relaxation) were observed in the intermediate frequency range of the frequency dependent dielectric loss plots. Anomaly peaks were observed in the temperature dependent dielectric constant curves. The shifting of the anomaly peaks towards higher temperature with the substitution of Ni suggested the increase in the antiferromagnetic ordering temperature. The complex impedance spectroscopic studies also showed relaxation effects which are non-Debye type. Moreover, this study predicted a typical negative temperature coefficient of resistance behaviour of these compounds. The intrinsic nature of the dielectric anomalies was also confirmed. Hence, it may be concluded that the dielectric anomalies were originated due to strong magnetoelctric coupling in these samples. A thorough study on the magnetic properties and magnetoelectric coupling of these ceramics is under progress.

**Reference**

1. Schmid, H.; Ferroelectrics 1994, 162, 317.
   **DOI:** 10.1080.00150199408245120
2. Wang, J.; Neaton, J.B.; Zheng, H.; Nagarajan, V.; Ogale, S.B.; Liu, B., Viehland, D.; Vaithyanathan, V.; Schlom, D.G.; Waghmare, U.V.; Spaldin, N.A.; Rabe, K.M.; Wuttig, M.; Ramesh,R.; Science 2003, 299, 1719.
   **DOI:** 10.1126/science.1080615
3. Wang, Y.; Nan, C.W.; Appl. Phys. Let. 2006, 89, 052903.
   **DOI:** 10.1063/1.2222242
4. Hill, N.A.; J. Phys. Chem. B. 2000, 104, 6694.
   **DOI:** 10.1021/jp000114x
5. Ederer, C.; Spaldin, N.A.; Phys. Rev. B. 2005, 71, 060401(R).
   **DOI:** 10.1103/PhysRevB.71.060401
6. Kubel, F.; Schmid, H.;Acta Crystallogr., sect. B: Struct. Sci. 1990, 46, 698.
   **DOI:** 10.1107/S0108768190006887
7. Yan, F.; On Lie, M.; Lu Li.; J. Phys. Chem. C. 2010, 114, 6994-6998
   **DOI:** 10.1021/jp1009127
8. Kumar, M.; Yadav, K.L.; J. Appl. Phys. 2006, 100, 074111.
   **DOI:** 10.1063/1.2349491
9. Feng, Y.N.; Wang, H.C.; Lue, SY.-D.; Hen, Y.; Lin, Y.-H.; J. Appl. Phys. 2013,113, 146101.
   **DOI:** 10.1063/1.4801796
10. Mandal, S.K.; Rakshit, T.; Ray, S.K.; Mishra, S.K.; Krishna, P.S.R.; Chandra, A.; J. Phys. : Cond. Matt. 2013, 25, 55303.
    **DOI:** 10.1088/0953-8984/25/5/055303
11. Pandit, P.; Pandit, P.; Satapathy, S.; Gupta, P.K.; Sathe, V.G. J. Appl.Phys. 2009, 106, 114105.
    **DOI:** 10.1063/1.3264836
12. Kumar, A.; Yadav,K.L.; J. Phys. Chem. of Solids 2011, 72, 1189-1194.
    **DOI:** 10.1016/j.jpcs.2011.06.006

13. Kumar, A.; Yadav, K.L.;Physica B 2010, 405, 4650-4654.
    **DOI:** 10.1016/j.physb.2010.08.054
14. Singh, S.K.; Palai, R.; Maruyama, K.; and, Ishiwara, H.; Elctrochem. Solid-State Lett. 2008, 11(7), G30.
    **DOI:** 10.1149/1.2912024
15. Wang, Y.H; Qi, X.; Procedia Engg. 2012, 36, 455-461.
    **DOI:** 10.1016/j.proeng.2012.03.066
16. Chaudhary, Y.A.; Mahajan, C.M.; Jagtap, P.P.; Bendre, S.T. J. Adv. Ceramics 2013, 2(2), 135-140.
    **DOI:** 10.1007/40145-013-0051-3
17. Wang, Y.; Xu, G.; yang, L.; Ren, Z.; Wei, X.; Weng, W.; Du, P.; Shen, G, Han, G. Mat. Science Poland 2009, 27(1), 219 – 224.
18. Cheng, Z.X.; Wang, X.L.; Du, Y.; Dou, S.X. J. Phys. D: Appl. Phys. 2010, 43, 242001.
    **DOI:** 10.1088/0022-3727/43/24/242001
19. Kharel, P.; Talebi, S.; Ramachandran, B., Dixit, A.; Naik, V.M.; Sahana, M.B.; Sudhaker,C.; Naik, R.; Rao, M.S.R.; Lawes, G. J. Phys. Condns. Matt. 2009, 21, 036001.
    **DOI:** 10.1088/0953-8984/21/3/036001
20. Qi, X.; Dho J.; Tomov, R.; Blamire, M.G.; Driscoll, J. L.M.; Appl. Phys. Lett. 2005, 86, 062903.
    **DOI:** 10.1063/1.1862336
21. Xu, J.; Wang, G.; Wang, H.; Ding, D.; He, Y.; Mater. Lett. 2009, 63, 855-857.
    **DOI:** 10.1016/j.matlet.2009.01.036
22. Karim, S.; Reaney, I. M.; Levin, I.; Sterianou, I.; Appl. Phys. Lett. 2009, 94, 112903.
    **DOI:** 10.1063/1.3097222
23. Sen, K.; Singh, K.; Gautam, A.; Singh, M.; Ceramics Int. 012, 38, 243-249.
    **DOI:** 10.1016/j.ceramint.2011.06.059
24. Kumar, M.; Yadav, K.L.; Appl. Phys. Lett. 2007, 91, 24290.
    **DOI:** 10.1063/1.2816118
25. Patil, D.R.; Lokare, S.A.; Devan, R.S.; Chougule, S.S.; Kanamadi, C.M.; Kokekar, Y.D.; Chugule, B.K.; Mater. Chem. Phys. 2007, 104, 254.
    **DOI:** 101016/jmatchemphys.2007.02.027
26. Chakrabarti, K.; Das, K.; Sarkar, B.; Ghosh, S.; De, S.K.; Sinha, G.; Lahtinen, J.; Appl. Phys. Lett., 2012, 101, 042401.
    **DOI:** 10.1063/1.4738992
27. Chang, F.; Zhang, N.; Yang, F.; Wang, S.; Song, G.; J. Phys. D: Appl. Phys. 2007, 40, 7799-7803.
    **DOI:** 10.1088/0022-3727/40/24/031
28. Kumar, M.; Yadav, K.L.; J. Phys.: Cond. Matt. 2006,18, L503-L508.
    **DOI:** 10.1088/0953-8984/18/40/L02
29. Pandit, P.; Satapathy, S.; Gupta, P.K.; Physica B 2011, 406, 2669.
    **DOI:** 10.1016/j.physb.2011.03.081
30. Cordero, F.; Ferretti , M.; Cimberle, M.R.; Masini, R.; Phys. Rev. B 2003,67, 144519
    **DOI:** 10.1103/PhysRevB.67.144519
31. Singh, H.; Yadav, K.L.; J. Phys.; Cond. Matt. 2011, 23, 385901.
    **DOI:** 10.1088/0953-8984/23/38/385901
32. Palkar, V.R.; Jhan, J.; Pinto, R.; Appl. Phys. Lett. 2002, 80, 1628.
    **DOI:** 10.1063/1.1458695
33. Uniyal, P.; Yadav, K.L.; J. Phys. Condens. Matter 2009, 21, 405901.
    **DOI:** 10.1088/0953-8984/21/40/405901
34. Karim, S.; Reaney, I.M.; Levin; I.; Sterianous I.; Appl. Phys. Lett., 2009, 94, 112903.
    **DOI:** 10.1063/1.3097222
35. Gautam, A.; Singh, K.; Sen, K.; Kotnala, R.K.; Singh, M.; J. Alloys Comp. 2012, 517, 87.
    **DOI:** 10.1016/j.jallcom.2011.12.025
36. Kumar, A.; Yadav, K.L.; Singh, H.; Pandu, R.; Reddy, P.R.; Physica B 2010, 405, 2362
    **DOI:** 10.1016/j.physb.2010.02.038
37. Mishra, R. K.; Pradhan, D.K.; Choudhary; R.N.P.; A. Banerjee, A.; J. Phys.: Cond. Matt., 2008, 20, 045218.
    **DOI:** 10.1088/0953-8984/20/04/045218
38. Mazumder, R.; Ghose, S., Mandal, P.; Bhattacharya, D.; Dasgupta, S.; Das, N.; Sen, A.; Tyagi, A.K.; Sivakumar, M.; Takami,T.; Ikuta, H.; J. Phys. 2006, 100, 33908.
    **DOI:** 10.1063/1.2229667
39. Catalan, G.; Scott, J.F.; Adv. Materials 2009, 21, 2463.
    **DOI:** 10.1002/adma.200802849.
40. Singh, H.; Yadav, K.L.;j. Phys.; Cond, Matt. 2011, 23, 385901.
    **DOI:** 10.1088/0953-8984/23/38/385901

41. Zhang, X.; Sui, Y.; Wang, X.; Mao, J.; Zhu, R.; Wang, Y.; Wang, Z.; Liu, Y.; Liu, W.; J. Alloys and Compd. 2011, 509, 5908-5912.
    **DOI:** 10.1016/j.jallcom.2011.03.037
42. Singh, H.;Kumar, A.; Yadav, K.L.;Mat. Sci. Engg. B 2011, 176, 540-547.
    **DOI:** 10.1016/j.mseb.2011.01.010
43. Sen, K.; Singh, K.; Gautam, A.; Singh, M.; Nanotech. And Nanosci. 2010, 1(1), 22-30.
44. Khatri, P.; Behera, B.; Srinivas, V.; Choudhary, R.N.P.; Res. Lett. Mat. Sc. 2008, 746256.
    **DOI:** 10.1155/2008/746256